X-Ray Diffraction Studies of 180° Ferroelectric Domains in $PbTiO_3/SrTiO_3$ Superlattices under an Applied Electric Field

P. Zubko,* N. Stucki, C. Lichtensteiger, and J.-M. Triscone

Department of Condensed Matter Physics, University of Geneva, 24 Quai Ernest-Ansermet, 1211 Geneva 4, Switzerland

(Received 24 November 2009; published 7 May 2010)

The dielectric response of $PbTiO_3/SrTiO_3$ superlattices is studied using electrical and structural measurements. While the dielectric response of paraelectric superlattices is well accounted for by the lattice contribution, superlattices with ferroelectric compositions exhibit an enhanced permittivity. X-ray diffraction allowed the presence of ordered nanodomains in ferroelectric superlattices to be established and their displacement under an applied bias to be directly probed, demonstrating that the enhanced permittivity in these artificial materials is due to domain wall motion.

DOI: 10.1103/PhysRevLett.104.187601 PACS numbers: 77.80.Dj, 61.05.C−, 77.84.Cg, 77.84.Ek

The functional properties of ferroic (ferroelectric, ferromagnetic, and ferroelastic) materials are highly influenced by their domain structure. As device dimensions shrink, so do the domains [1], leading to extremely dense domain patterns at the nanoscale. The continuing drive for device miniaturization and progress in thin film synthesis have sparked a new wave of research on nanodomains. Recent theories, for instance, predict rather unusual polarization profiles and domain dynamics in ferroelectric thin films and superlattices [2,3], which are yet to be tested experimentally. At the same time, part of the focus is shifting to domain walls—the boundaries between domains—as new experimental and theoretical work has revealed that they often possess fascinating structural and electronic properties of their own, opening an exciting possibility for novel devices based on the concept of domain wall engineering. Recent examples include the discovery that domain walls in multiferroic $BiFeO_3$ are conducting and can be used to obtain above-band-gap photovoltaic responses [4].

Probing the electrical properties of nanodomains in ultrathin films is rather challenging. Even local scanning probe techniques, which have been invaluable in studying domain dynamics in thin ferroelectrics [5], do not always have sufficient resolution (limited by the tip radius). Macroscopic techniques, such as x-ray diffraction, have been successfully used to image regular periodic 180° domain patterns in ultrathin ferroelectric films [6], but nonzero field studies are hindered by the conductivity of such thin samples. In this Letter, we show that $PbTiO_3/SrTiO_3$ (PTO/STO) ferroelectric-paraelectric superlattices provide an ideal system for studying, using x-ray diffraction, the response of ferroelectric nanodomains to uniform electric fields and that the enhanced dielectric properties observed in such ferroelectric superlattices are linked to nanoscale domain wall motion.

PTO/STO superlattices have already proven to be an exciting system, offering a way of creating new artificial materials with desirable properties that can be easily tuned by simply changing the various layer thicknesses [7]. Furthermore, the PTO/STO interfaces were found to host a novel coupling between the ferroelectric mode and antiferrodistortive rotations of the oxygen octahedra, giving rise to improper ferroelectricity [8]. In this Letter we study the nanodomain structure of PTO/STO superlattices and for simplicity restrict our attention to long-period superlattices where interface effects are less important.

To allow dielectric measurements to be performed, the superlattices were sandwiched between ~30 nm thick conducting $SrRuO_3$ (SRO) electrodes. The PTO and STO layers were grown by off-axis radio frequency magnetron sputtering on TiO_2 terminated (001) STO substrates in a 0.18 Torr oxygen/argon atmosphere of ratio 14:32 with a substrate temperature of 520 °C (the corresponding parameters for SRO are 0.1 Torr, 3:40, and 650 °C). Figure 1(a) compares the polarization for different PTO volume fractions x of two series of superlattices: one with SRO top and bottom electrodes (filled circles) and the other (open squares) grown on conducting Nb-doped STO substrates and with Au top electrodes [7]; x is defined as $x = n_{PTO}/(n_{PTO} + n_{STO})$ where n_{PTO} and n_{STO} are the number of unit cells of PTO and STO in a superlattice period. The macroscopic remnant polarization P_r, as measured by the PUND (positive up negative down) technique [7], is in good agreement with the Landau-Devonshire (LD) theory prediction (solid line) for superlattices on Nb-STO, whereas samples with SRO electrodes show almost zero remnant polarization for all but the highest PTO volume fractions. In contrast, the structural parameters such as the tetragonality were found to be almost identical for the two series, indicating that the intrinsic microscopic spontaneous polarization (P_s) values are the same.

Figure 1(b) shows the room temperature dielectric constants for the superlattices with SRO electrodes, together with the LD prediction [7] calculated for different applied electric fields as a function of the PTO volume fraction. The vertical dotted line indicates the critical PTO volume fraction x_c separating ferroelectric superlattices ($x > x_c$) from paraelectric ones ($x < x_c$). As can be seen, for com-

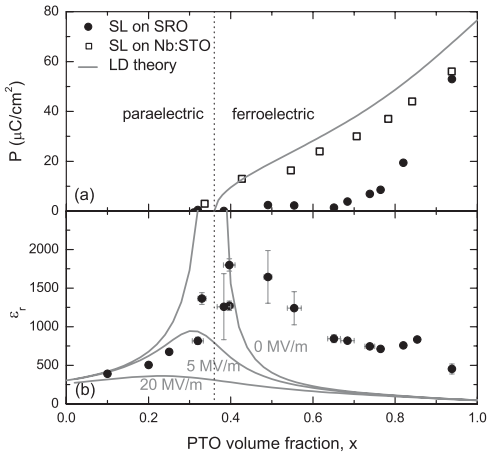

FIG. 1. (a) Room temperature polarization for different compositions x revealing the suppression of remnant polarization in superlattices (SLs) with SRO electrodes (filled circles), in contrast to samples grown on Nb-doped STO substrates (open squares), which show good agreement with the LD theory prediction (solid line [7]). (b) Dielectric constants for superlattices with SRO electrodes together with theoretical predictions for different fields (solid lines). The dashed vertical line represents the critical PTO volume fraction x_c separating paraelectric ($x < x_c$) and ferroelectric ($x > x_c$) compositions. Ferroelectric samples show ϵ_r values way above those expected from lattice contributions alone, suggesting that other mechanisms, such as domain wall motion, may be contributing.

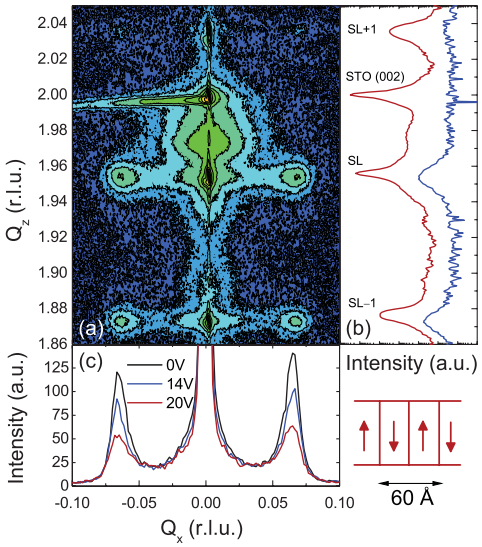

FIG. 2 (color). (a) Reciprocal space map showing the substrate STO (002) reflection and three clear superlattice (SL) peaks, each with two broad satellite peaks due to 180° ferroelectric domains (period ≈ 60 Å). (b) Intensity profiles along two crystal truncation rods: through the main Bragg peaks at $Q_x = 0$ (red) and through the domain satellite peaks (blue). (c) Domain satellites under different applied fields recorded around the main SL peak. Reciprocal lattice units (r.l.u.) are defined with respect to the substrate lattice parameter $a = 3.905$ Å.

positions that are paraelectric, the relative dielectric constants (ϵ_r) are in good agreement with the values expected for the lattice response (the LD prediction), indicating that extrinsic contributions such as free carrier injection, space charge, or interface effects are not important. The field dependence of ϵ_r for the STO rich samples ($x \ll x_c$) was also found to be in excellent agreement with LD theory predictions. The permittivities of the ferroelectric superlattices, however, are up to an order of magnitude larger than the expected intrinsic dielectric response of the lattice. This, together with the suppression of remnant macroscopic polarization (despite no change in tetragonality), is suggestive of a polydomain state with domain wall motion responsible for the large increase in permittivity. Similar permittivity enhancements were reported for the low temperature rhombohedral phase of $BaTiO_3$ single crystals, and attributed to domain wall sliding [9].

Domains in superlattices have been inferred by a number of groups, e.g., [10,11], and have already received significant attention from the theoretical community, e.g., [3,12]. The presence of ferroelectric domains in our samples for $x > x_c$ was confirmed by x-ray diffraction measurements. Figure 2 shows satellites around the superlattice Bragg peaks, typical of periodic domain structures [6,13]. The satellites were present around all (00L) and (H0L) Bragg peaks examined and were observed to disappear above the ferroelectric-paraelectric phase transition temperature, confirming that they originate from ferroelectric domains. Only first order satellites were observed, most likely due to significant variation of domain sizes [14]. For the sample investigated in Fig. 2, with 8 uc PTO and 4 uc STO repeated 100 times, the periodic domain structure has a wavelength equal to about 60 Å.

A detailed analysis of the domain structure will be presented elsewhere. Here we will concentrate on the unique opportunity offered by $PbTiO_3/SrTiO_3$ superlattices to study nanodomains under applied electric fields using x-ray diffraction. The small lattice parameter mismatch between these two materials allows coherent growth of structures with total thicknesses of hundreds of nanometers without relaxation, hence keeping a high material perfection. These samples seem thus ideal for x-ray experiments where one wants to apply large voltages to large area electrodes without significant leakage problems. The x-ray measurements were performed using a PANalytical X'Pert PRO diffractometer on approximately 2×2 mm^2 superlattices with SRO electrodes covering the entire top surface (apart from the very edges to avoid electrical shorting). Reciprocal space line scans along the in-plane direction (Q_x) were obtained by recording the rocking curves around the superlattice (00L) Bragg peaks. The results presented have been reproduced on several other samples.

An Agilent 4284A precision LCR meter was used to apply the dc bias across the sample, while at the same time recording the ac capacitance and dielectric loss tangent (10 mV, 1 kHz signal used). The dc bias produced two

effects on the measured diffraction pattern. First, the superlattice peaks shifted to lower 2θ values, indicative of an increase in the average lattice parameter, while the Bragg peaks from the substrate and SRO electrodes remained unchanged. This was interpreted as a simple piezoelectric effect. By quantifying the changes in the lattice parameter we were able to extract effective piezoelectric coefficients of several tens of pm/V for the samples investigated, comparing quite well with independent measurements using a scanning tunneling microscope on superlattices of the same composition [15]. Second, the peak intensities of the domain satellites were observed to decrease with increasing bias without changes in the peak positions, as shown in Fig. 2(c). The leakage currents were monitored at all times by a series ammeter and great care was taken to ensure that the observed effects were not due to temperature changes induced by the power dissipated in the sample. The intensity modulations were reversible with a recovery observed when the field was reduced to zero again. This implies that the domain walls return to more or less their original positions despite the long duration (up to several hours) of the applied voltage, and is consistent with the very small value of the remnant polarization.

There are a number of possible ways domains can respond to an external field. Pure electrostatic considerations suggest that the thermodynamic ground state under an applied bias corresponds to a domain structure with a period larger than that at zero field [16]. This is not observed experimentally. Such a change in domain period requires the collective motion of domain walls over macroscopic distances, or appropriate creation and annihilation of domain boundaries, and is energetically very costly. A simpler, less costly, response to an electric field is a change in the sizes of oppositely polarized domains without a change in periodicity. This involves only local microscopic motion of domain walls within each domain period. Unlike in bulk crystals or thick films, where switching requires large and generally irreversible domain wall displacements, in the case of nanodomains, large changes in polarization can be obtained from tiny wall displacements. In the sample investigated the domain walls are separated by ~30 Å; hence, each wall need only move 15 Å (i.e., ~4 uc) to fully saturate the polarization. Pinning by defects is likely to play an important role as the relative changes in domain sizes may be achieved through the reversible bending of domain walls around pinning centers rather than by the displacements of the wall as a whole.

To gain some physical insight into the observed field-induced intensity modulations, we shall consider a simplified model where the domain structure is represented as a rectangular wave of period $2l$. This can be expressed as

$$F(x) = \sum_{n=-\infty}^{\infty} \delta(x - n2l) \otimes T(x, a), \tag{1}$$

where $\otimes$ represents the convolution operation, $2a$ is the size of (say) the "up" domains, and $T(x, a)$ is the top-hat function equal to 1 for $-a \leq x \leq a$ and zero elsewhere. The diffraction pattern of (1) is given by its Fourier transform

$$\tilde{F}(q) = \frac{1}{\sqrt{2\pi}} \sum_{n=-\infty}^{\infty} e^{-in2lq} \sqrt{\frac{2}{\pi}} \frac{\sin aq}{q} \tag{2}$$

which is a product of two terms. The first term originates from the total domain periodicity ($2l$) and hence defines the positions of the satellites, which appear at $q = \frac{m\pi}{l}$, where m are integers. The second term modulates the intensities of these peaks according to the volume fraction of the up domains $f = a/l$. One can see that when $a = \frac{l}{2}$, i.e., the sample has an equal fraction of up and down domains, all peaks with even values of m disappear and that the peaks with odd m have maximum intensity. In the presence of a field, the relative domain sizes change and hence the intensities of the odd m peaks decrease whereas those of the even peaks increase according to

$$\frac{I_m(a)}{\max[I(a)]} \equiv \frac{I}{I_0} = \sin^2\left(\frac{ma\pi}{l}\right) = \sin^2(mf\pi). \tag{3}$$

The domain fraction f can be estimated from electrical measurements, which were performed on an identical sample but with the top SRO layer patterned into 120×120 μm^2 electrodes. The measured dielectric response and polarization-voltage (P-V) loop are shown in Figs. 3(a) and 3(b). Ignoring other possible contributions (e.g., from space charge layers or injected carriers), the increase in polarization from local polarization reversal due to domain wall motion P_d can be obtained by simply subtracting the nonswitching contribution P_{diel} (i.e., that due to the field-induced intrinsic dielectric response) from the total measured polarization. We estimate the contribution of P_{diel} from LD theory, approximating the intrinsic dielectric response of both the up and down domains with that of a monodomain superlattice having a polarization aligned parallel to the applied field [i.e., the bold part of the red curve in Fig. 3(a)]. The calculated P_{diel} is plotted in red in Fig. 3(b). The up-domain fraction [Fig. 3(c)] can now be calculated using $f(V) = \frac{1}{2}[(P_d/P_s) + 1]$, where the LD theory value for P_s is 34.1 μC/cm^2 for this composition. Further details regarding the calculation of P_{diel} and the approximations involved can be found online [17]. Here we only point out that the LD description of the intrinsic dielectric response is not perfect, as is clear from the fact that a full polarization reversal is not observed in our samples despite exceeding the thermodynamic coercive voltage, indicated by the divergence of ϵ_r in Fig. 3(a). The inadequacy of our simple LD theory model developed for monodomain samples in accurately describing the contribution from the intrinsic dielectric response is in part due to the dense domain structure itself. It was recently shown by Chen and Roytburd [18] that electromechanical con-

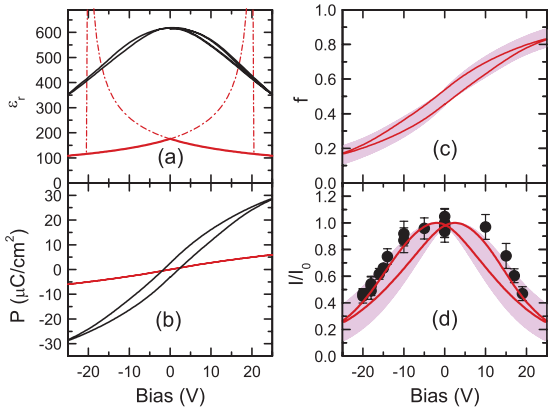

FIG. 3 (color). (a) Measured dielectric response (black) compared with a theoretical curve expected for a monodomain sample of the same average composition x (red); the dielectric loss, $\tan\delta$, was below 0.008 over the entire range of biases. (b) Polarization-voltage hysteresis curve (black) and the approximate lattice contribution to the polarization (red) estimated from LD theory. (c) The "up"-domain fraction calculated from the measured P-V loop and the LD predictions for P_{diel} and P_s. (d) The observed intensities of domain satellite peaks (data points) normalized to the zero bias value and compared with the prediction of Eq. (3). Shaded regions illustrate the effect of a $\pm 5\ \mu\mathrm{C/cm}^2$ variation in P_s.

straints at domain boundaries lead to interdomain clamping, effectively stiffening the lattice as well as hindering complete switching.

With the above caveats, the calculated $f(V)$ was used to estimate the expected changes in intensity of the first order satellite peaks for different applied voltages using Eq. (3) [red curve in Fig. 3(d)]. For comparison, the actual intensities of the satellite peaks (these are intensities at peak maxima, normalized to the value at zero volts [19]) are plotted as filled circles. The agreement is excellent, implying that the observed intensity changes are consistent with local domain rearrangements which alter only the relative domain sizes but not the domain period (as the latter would show up as a change in the satellite peak positions). A decrease in satellite intensities could also result in part from an increase in domain randomness (domain size variation) [14], a point that should be studied further. These results allow important conclusions to be drawn. While subjected to large electric fields, in excess of the thermodynamic coercive field, for very long times, the system does not reach a monodomain configuration. Instead the relative sizes of oppositely poled domains change with field via domain wall motion but without annihilation of domains walls. When the field is reduced, the original domain structure is restored. The nanoscale domain wall motion (of the order of 10 Å or a few unit cells for the largest applied fields) is at the origin of the enhanced permittivity observed in these artificial materials.

In conclusion, we have shown that PTO/STO superlattices present an appealing system for the study of ordered 180° nanodomains under an applied field, enabling simultaneous electrical and structural measurements to be performed on large samples. With the low intensity laboratory x-ray source used here, only static properties could be probed. On the other hand, synchrotron radiation equipped with current detectors that allow nanosecond time resolution opens new exciting possibilities of studying with x rays the dynamics of periodic domain structures at the nanoscale [20].

The authors thank S. Gariglio, G. Calatan, and M. Dawber for helpful discussions, and acknowledge funding from the Swiss National Science Foundation through the NCCR MaNEP and division II, and the EU project OxIDes.

*Electronic address: pavlo.zubko@unige.ch

[1] L. Landau and E. Lifshitz, Phys. Z. Sowjetunion **8**, 153 (1935); C. Kittel, Phys. Rev. **70**, 965 (1946).
[2] I. A. Luk'yanchuk, L. Lahoche, and A. Sené, Phys. Rev. Lett. **102**, 147601 (2009).
[3] S. Lisenkov, I. Ponomareva, and L. Bellaiche, Phys. Rev. B **79**, 024101 (2009).
[4] J. Seidel *et al.*, Nature (London) **8**, 229 (2009); S. Y. Yang *et al.*, Nature Nanotech. **5**, 143 (2010).
[5] P. Paruch, T. Tybell, and J.-M. Triscone, Appl. Phys. Lett. **79**, 530 (2001).
[6] D. D. Fong *et al.*, Science **304**, 1650 (2004).
[7] M. Dawber *et al.*, Adv. Mater. **19**, 4153 (2007).
[8] E. Bousquet *et al.*, Nature (London) **452**, 732 (2008).
[9] Y. L. Wang, A. K. Tagantsev, D. Damjanovic, and N. Setter, Appl. Phys. Lett. **91**, 062 905 (2007).
[10] E. D. Specht, H.-M. Christen, D. P. Norton, and L. A. Boatner, Phys. Rev. Lett. **80**, 4317 (1998).
[11] Y. L. Li *et al.*, Appl. Phys. Lett. **91**, 112 914 (2007).
[12] V. A. Stephanovich, I. A. Luk'yanchuk, and M. G. Karkut, Phys. Rev. Lett. **94**, 047601 (2005).
[13] Similar domains were at the same time observed in pulsed laser deposition prepared $PbTiO_3/SrTiO_3$ superlattices by Ard H. G. Vlooswijk, Ph.D. thesis, University of Groningen, 2009.
[14] R. Takahashi, Ø. Dahl, E. Eberg, J. K. Grepstad, and T. Tybell, J. Appl. Phys. **104**, 064 109 (2008).
[15] N. Stucki, Ph.D. thesis, University of Geneva, 2008.
[16] A. Kopal *et al.*, Ferroelectrics **223**, 127 (1999).
[17] See supplementary material at http://link.aps.org/supplemental/10.1103/PhysRevLett.104.187601 for details of the calculation of the domain fraction f.
[18] L. Chen and A. L. Roytburd, Appl. Phys. Lett. **90**, 102 903 (2007).
[19] Integrated intensities show similar behavior but suffer from larger errors due to difficulties in adequate background subtraction.
[20] A. Grigoriev *et al.*, Phys. Rev. Lett. **96**, 187601 (2006).